Reduction and control of domain spacing by additive inclusion: Morphology and orientation effects of glycols on microphase separated PS-b-PEO

Tandra Ghoshal,[1,2*] Matthew. T. Shaw,[3] Justin D. Holmes,[1,2] Michael A. Morris[1,2*]

[1]Materials research group, Department of Chemistry and Tyndall National Institute, University College Cork, Cork, Ireland,

[2]AMBER (Advanced Materials and Biological Engineering Research Centre), Trinity College Dublin, Dublin, Ireland,

[3]Intel Ireland Ltd., Collinstown Industrial Estate, Co. Kildare, Ireland

[*] Corresponding Author: Prof. Michael A. Morris

Tel: + 353 21 490 2180

Fax: +353 21 427 4097

E-mail: m.morris@ucc.ie

*Dr. Tandra Ghoshal

Tel: + 353 21 490 2911

Fax: +353 21 427 4097

E-mail: g_tandra@yahoo.co.in

ABSTRACT: Cylindrical phase polystyrene-b-polyethylene oxide (PS-b-PEO) block copolymer (BCP) was combined with lower molecular weight poly/ethylene glycols at different concentrations and their effect on the microphase separation of BCP thin films were studied. Well-ordered microphase separated, periodic nanostructures were realized using a solvent annealing approach for solution cast thin films. By optimizing solvent exposure time, the nature and concentration of the additives etc. the morphology and orientation of the films can be controlled. The addition of the glycols to PS-b-PEO enables a simple method by which the microdomain spacing of the phase separated BCP can be controlled at dimensions below 50 nm. Most interestingly, the additives results in what might be expected increase in domain spacing (i.e. pitch size) but in some conditions an unexpected reduction in domain spacing. The pitch size achieved by modification is in the range of 16-31 nm compared to an unmodified BCP system which exhibits a pitch size of 25 nm. The pitch size modification achieved can be explained in terms of chemical structure, solubility parameters, crystallinity and glass transition temperature of the PEO because the additives act as PEO ‘stress cracking agents’ whereas the PS matrix remains chemically unaffected.

Keywords: self-assembly. block copolymer. domain spacing reduction. additives and glycols. morphology and orientation.

1. Introduction

The continual reduction of critical dimensions (CDs) of advanced semiconductor devices challenges conventional ultraviolet (UV) lithography and requires the use of new and alternative patterning techniques such as double or triple patterning to create substrate features for use in both logic and memory device and interconnect level circuitry [1]. Advances in extreme UV lithography technology have proven to be slow, complex and expensive. Directed self-assembly lithography (DSAL) is being explored as viable bottom-up patterning technique for next generation lithography in making both hole [2] and line/space patterns [3]. Potentially, DSAL offers an industry integratable patterning solution in a cost-effective, robust and scalable manner. The most promising and advanced of the DSA techniques for lithography is the microphase separation of BCPs which form a number of highly regular nanostructured morphologies by a process known as microphase separation arising from the chemical incompatibility of the blocks [4-7]. For many types of BCPs, exposure to solvent atmospheres at elevated temperatures (solvent annealing) is an efficient approach for microdomain ordering and orientation in short time periods [8-9]. Here, a solvent swells the polymer, creating free volume (i.e. effectively a reduction in glass transition temperature of the polymer) and allowing the necessary chain mobility for the polymer blocks to phase separate and facilitate self-assembly into distinct microdomains [8, 10]. Achieving ultra-small pitch sizes by DSA is a challenge since the domain dimensions are determined by the random coil size and, hence, the molecular weight of the BCP. Since the period (pitch) dimension of the BCP microdomains scale as approximately 2/3 power of the molecular weight, achieving sub-15 nm feature size requires the use of very low molecular weight BCPs [11]. Synthetic control of polymer molecular weight is still very challenging, and molecular weight variations of 10-15% are uncommon in current DSA polymer synthesis. There is, therefore, a strong motivation to develop and understand methods that

allow tuning of the domain size of established BCP systems to meet the CD and pitch specifications required for practical implementation in the micro-nanoelectronics industry.

Blending (i.e. use of additives) at the molecular level is an effective means of tailoring both BCP morphology and microstructural dimensions which depend on the ratio of the molar weight, volume fractions and miscibility of the additive in the BCP [12-14]. Morphological and microdomain size adjustment has been studied for various homopolymers and surfactant blends as well as the attachment of small molecules to the block copolymers [13, 15-19]. In general, the pitch size increases or is unaltered by molecular additives depending on the chain distribution of the additive within the microdomains of the BCP [20-22]. This latter point is of importance since the additive distribution in the BCP strongly depends on the chemical environment and, as a result, the solvent annealing process [23]. At larger additive concentrations, it might be expected that additives will act as solvent molecules and have distinct effects on morphology and dimension of the BCP [24].

Guided by previous studies, [18, 20-22] this work will quantify the influence of an additive of similar chemical structure to one of the BCP blocks and study the effects of small block length glycols on the microphase separation of PS-b-PEO, a system that has been shown to be modifiable by addition of homopolymers etc. In this research, we have studied the behaviour of thin films of mixtures of cylindrical phase BCP's and poly/ethylene glycols and tuned the experimental parameters to significantly influence both the microdomain cylinder orientation (i.e. morphology) and the domain dimension for possible use in lithographic applications [25-27]. The results show that structural dimension (i.e. domain spacing or pitch) could be effectively and controllably reduced by addition of these simple additives.

2. Experimental section

Materials. The BCP PS-b-PEO was purchased from Polymer Source and used without further purification (number-average molecular weight, M_n, PS = 16 kg mol^{-1}, M_n, PEO = 5

kg mol^{-1}, M_w/M_n = 1.04, M_w: weight-average molecular weight). The additives ethylene glycol (EG, M_w: 62.07), triethylene glycol (TEG, M_w: 150.17) and poly(ethylene) glycol (PEG, M_w: 1500) and the solvent toluene were purchased from Sigma Aldrich. Single crystal (100) boron doped (P type) silicon wafers with a native silica layer were used as the experimental substrates.

Procedure. Substrates were cleaned by ultrasonication in acetone (30 min) and toluene (30 min) and dried under nitrogen. A 1 wt% (all compositions as w/w) PS-b-PEO solution in toluene was stirred for 12 h at room temperature. Different weight compositions of the glycols were added and solutions stirred at room temperature for 12 h. The resultant solution was spin coated onto the substrate at 3000 rpm for 30 s. The films were exposed to toluene vapour placed at the bottom of a closed vessel kept at 50^0C for different time period to induce microphase separation. After solvent annealing for the desired time, the films were dried under nitrogen stream.

Characterizations. Surface morphologies were imaged by scanning probe microscopy (SPM, Park systems, XE-100) in tapping mode and scanning electron microscopy (SEM, FEI Company, FEG Quanta 6700 and Zeiss Ultra Plus). The film thicknesses were measured by optical ellipsometer (Woolam M2000) and electron microscopy (i.e. cross-sections). Partial etching of PEO was carried on a STS dry etching system (Advanced Oxide Etch (AOE) ICP etcher) using an SF_6/O_2 gas mixture. Sample cross-sections were prepared for the Transmission electron microscopy (TEM) using an FEI Helios Nanolab 600i system containing a high resolution Elstar™ Schottky field-emission SEM and a Sidewinder FIB column. These were then imaged by TEM (JEOL 2100). Fourier Transform Infrared Spectrometry (FTIR) spectra were recorded on infrared spectrometer (IR 660, Varian).

3. Results and discussion

3.1. Morphological evolution of PS-PEO/ethylene glycol thin film

The morphology of the thin films prepared by PS-b-PEO-EG mixtures following solvent annealing in toluene at 50^{o} C for different periods of time with different compositional ratio was studied. The coating solutions were transparent with up to 50% EG content composition indicating the macroscopic homogeneity of the mixture. Above this concentration the solutions were obviously translucent at room temperature. Fig. 1 shows representative tapping mode AFM images demonstrating the morphological and size variation of the solvent annealed films prepared with an EG weight fraction of 20%. This BCP without the addition of any EG forms a hexagonally ordered cylindrical morphology dot patterns with an average centre to centre microdomain spacing of 25 nm after solvent annealing in toluene/water for 1 hour [9]. As-cast films with the glycol addition possess a disordered morphology without little indication of feature periodicity. Solvent annealing results in the formation of hexagonally ordered dot patterns of vertically orientated PEO microdomains (PEO cylinders are darker in colour in the AFM image) within the PS matrix. Note that thermal annealing at the same temperature in the absence of the solvent has little effect on the as-cast disordered structure demonstrating that toluene is a necessary component to induce phase separation. The films are of uniform thickness across the substrate area. No dewetting or phase transitions were observed for annealing between 30 min and 3 h. The ellipsometry measured film thicknesses varied cyclically between 35 to 40 nm with the annealing time. The observed thickness variation corresponds to repeated swelling and deswelling effects of the film with solvent annealing in the toluene environment as noted before [8]. The corresponding average centre to centre distances between adjacent microdomains decreased from 25 nm to 16 nm with annealing time (Figs. 1a-f). Significant non-uniformity in PEO cylinder diameters as well as in pitch sizes were noticed over the annealing period. This non-uniformity stabilizes with time (See supporting Information, Fig. S2a). Table 1 summarizes the morphology and pitch size variation of the solvent annealed films for different concentrations of additives with

annealing time. Note, only a small thickness variation across the surface was observed at annealing periods > 2 h. No significant deviation of the film thickness and morphology was observed with increasing EG content up to 40%. However, significant film dewetting and thickness variation was observed for 70% EG composition (See Supporting Information, Fig. S1). The large scale ordering, size uniformity, periodicity and pitch size variability suggests that this BCP EG mixing may be a means to control feature size without changing the actual molecular weight of the BCP.

3.2. Morphological evolution of PS-PEO/Tri-ethylene glycol thin film

A similar approach used as for the PS-PEO/ethylene glycol mixture was carried out for the PS-b-PEO/TEG (20%) system in order to examine the morphological and pitch size variation effects. As above, hexagonally arranged vertically orientated cylinder arrangements were observed across the substrate after solvent annealing under toluene vapour. However, in the 20% PS-b-PEO/TEG system, the structures formed have noticeably more defects compared to the analogous EG systems. The average centre to centre distances between cylinders decreases from 25 nm to 20 nm with annealing time (Figs. 2a-f). Note also that significant variation in PEO microdomain diameter and thickness undulation was observed compared to the EG systems (See Supporting Information, Fig. S2(b)). The average ellipsometric measured thicknesses decreased gradually from 45 nm to 35 nm with annealing time. These results suggest that the lower molecular weight EG molecule (TEG) was less uniformly distributed and reacted within the BCP nanostructure during the solvent annealing process. No nanostructure was obtained on increasing the TEG content (>20%) which might suggest a solubility limit of TEG within the BCP. The excess TEG formed a separate layer on top of the film surface as evident from rather featureless microscopic image (not shown).

3.3. Morphological evolution of PS-PEO/PEG thin film

The changes in morphology and feature size of the PS-PEO 20% PEG thin film system as a function of solvent anneal time are described in Fig. 3. A well ordered arrangement of perpendicularly orientated PEO cylinders was observed across the substrate surface after solvent annealing in toluene for 30 min (Fig. 3a). The average microdomain spacing is 27 nm. Increasing the annealing time to 1h results in a hybrid morphology consisting of cylinders oriented both parallel and perpendicular to the surface plane as shown in Fig. 3b. A transition to a parallel cylinder orientation was observed following anneal periods of 1.5 and 2 h respectively (Figs. 3c and d). Further annealing provides firstly mixed then vertical cylinder orientations (Figs. 3e and f). Further annealing still resulted in gross dewetting preventing additional study. The average centre to centre cylinder spacing increases from 27 nm to 31 nm for the annealing time of 3h. The phase separated films exhibit lower defect densities and smoother surface compared to the films with smaller (EG, TEG) glycols after similar treatments (See Supporting Information, Fig. S2(c)). The films formed had uniform thickness across the substrate which varied cyclically between 40-45 nm with anneal time. Note that, films with no observable nanostructures consisting of an upper PEG layer (as evident from the microscopic image) were obtained either by increasing the amount of PEG content or by increasing the molecular weight of PEG. The modification of CD's and surface morphologies for the PS-PEO thin films can thus be controlled carefully by mixing different chain length EG/PEG's in the polymer solution without changing the parent BCP system.

3.4. Morphology and interfaces by SEM and cross sectional TEM

The AFM images clearly demonstrate the surface morphology of the films, however, the internal structure is unknown. The similarity of the PS and amorphous PEO densities (1.05 g cm^{-3} and 1.12 g cm^{-3} respectively) [28] prevent good quality electron imaging. This suggests that solvent annealing does not result in PEO crystallization since the crystalline form has higher density (1.24 g cm^{-3}) [29] and might be expected to provide microscopic contrast [30].

In order to induce block contrast, a plasma dry etch process was applied to partially remove the PEO domains. SEM and cross-sectional TEM analysis for the sample solvent annealed for 3 h with EG content of 20% are shown in Fig. 4 and Fig. 5 respectively. The SEM image (Fig. 4a) demonstrates highly periodic, hexagonally arranged, dot patterns with a 16 nm domain spacing, similar to AFM data from unetched samples (Fig. 1f). The periodicity of the array can easily be seen and is consistent with an ideal hexagonal packing of the cylindrical domains. Note that cross sectional SEM images (Fig. 4b) suggest that the etch used had limited etch selectivity (PEO:PS) as it resulted in a reduction of the film thickness to 25 nm from its original value of 35 nm. But the structural arrangement remained unaltered. The bottom surface of the film is intact with the substrate and has same structure as the top, which implies the cylindrical domains span the entire film thickness.

The internal morphology was further analysed by cross sectional TEM to provide further detail. Fig. 5 show the rippled, wave-like arrangement resulting from the low selective partial etch of the PEO block. The average spacing of features was consistent with a domain spacing of 16 nm in agreement with SEM. Note the surface rippling is not perfectly sinusoidal because of either etch inhomogeneity and/or a non-perfect image projection (since the film may not have been cut exactly orthogonal to the dots). A higher magnification image (Inset of Fig. 5) revealed the average diameter of the PEO domain was 8 nm, which were broadened during the etching step. The film was well adhered to the substrate surface with no indication of deformation or delamination.

3.5. Compositional analysis by FTIR

FTIR spectroscopy was used here to provide information regarding intermolecular interactions corresponding to stretching or bending vibrations of particular bonds. The positions at which these peaks appear in the FTIR spectra depend directly on the bond strength. The spectroscopy also used to confirm the presence of residual or trapped solvent in

the phase separated nanostructured thin films. Fig. 6 shows representative FTIR spectra of the BCP thin films after solvent annealing for 3h prepared with three different additives (EG, TEG, PEG) at a compositional content of 20% each. All the spectra recorded display features typical of the PS and PEO blocks. Peaks around 743 cm^{-1} (benzene bending), 1602 cm^{-1}, 1494 cm^{-1} and 1462 cm^{-1} (benzene ring stretching), weak overtone and combination bands in the range of 1655-2000 cm^{-1} can all be attributed to polystyrene [31]. The features at 1106 cm^{-1} (C-O-C stretch), 931 cm^{-1} (CH_2 PEO rocking modes), and 1749 cm^{-1} and 1720 cm^{-1} (C=O stretches of the ester and keto group respectively) as well as peaks at 2910 cm^{-1} and 2872 cm^{-1} (CH_2 PEO stretching modes) can all be assigned to the PEO block [32]. For the EG modified films, no residual EG was detected for the films annealed for longer time implying complete dissolution/reaction of EG within the BCP. Note that neat EG is characterized by the absorption bands due to the C-C-O stretching at 1087 and 1044 cm^{-1} and symmetric and asymmetric C-H stretching bands at 2874 and 2941 cm^{-1}, which are absent [33]. Further, no O-H stretching vibration bands are detected. The bands corresponding to glycols were detected for the TEG modified films. A broad intense band was also seen due to the OH stretching vibration between 3100-3600 cm^{-1}. The important vibrations detected in the spectrum for the PEG modified films were the C-H stretching at 2874 cm^{-1}, C-O stretching at 1104 cm^{-1} and OH stretching centred at 3300 cm^{-1} [34]. On the basis of this FTIR data it might be argued that lower molecular weight EG is not only well-distributed throughout the BCP, but it has also modified the BCP such that it leads to uniform pitch size throughout the film surface with no residual or trapped solvent being detected. For the TEG and PEG systems the results suggest that they are reacted partly, thus, the environments are similar to those in their normal state and local pitch size variation is expected.

3.6. Mechanism: Microphase separation and pitch modification

On the basis of these data it can be convincingly argued that the lower molecular weight EG is well-distributed throughout the BCP. Note that for the EG 20% system, a narrow size/spacing distribution was observed after annealing for the longest periods suggesting homogeneous distribution of EG. For TEG and PEG, the data suggest limited solubility since the FTIR glycol peaks are visible after solvent annealing. However, some material is dissolved in the block since there are domain spacing changes observed. Note that the size/spacing distribution is broader than might be expected suggesting a very inhomogeneous distribution. The FTIR data suggest that no residual or trapped solvent could be detected confirming the effects observed are not due to significant solvent incorporation and retention following solvent annealing. For the TEG and PEG systems the data indicate some of the molecules are incorporated into the PEO block but the solubility is less than that for EG and an inhomogeneous distribution of the molecules exists.

Explaining a basis for these effects is complex as the introduction of small molecules into a BCP film can affect the system by more than simple swelling of the block(s). Here, it can be assumed that the additives are molecular additives. This is possible because while stirring, the polyethylene oxide block and the EG do not react with each other at room temperature [35] and chemical condensation of the glycols and the PEO blocks is limited by mass transport (segregation/diffusion etc.) and can only occur during the solvent annealing processes. When these molecular units enter the BCP system, it is likely to affect the structure and dimension of the microphase separated structure since these are determined by a balance between the packing and interfacial free energies at thermodynamic equilibrium so as to minimize the interfacial energy between blocks. This enthalpic driving force is balanced by the chain stretching and lower domain packing density resulting from block-block repulsion [36]. In this work, we did not attempt to modify the polymer-substrate interactions by e.g. use of brush layers. This balance of the inter-block forces ensure that the additive will affect the

system by more than simple swelling of the block(s) since these forces will be altered by the presence of these molecules. There is a further layer of complexity since the PS-b-PEO system is heterogeneous as the blocks exhibit asymmetric affinities for the solid substrate and the air interface. Previous work suggests that the hydrophilic PEO will preferentially wet the substrate surface (favourable PEO-substrate interactions) whilst PS will segregate to the air interface to form a PS-rich layer (PS has a lower surface energy, γ_{PS} = 33 mNm^{-1}; γ_{PEO} = 43 mNm^{-1}) [37].

When a molecule/short polymer chain of similar chemical structure to one of the blocks (so that it is trapped within that block) is added in a small amount to a microphase separated BCP, there is a partial decoupling of the interfacial free energy and the packing free energy [36]. The small polymer chains are trapped in the domains of the corresponding block of the BCP and establish an equilibrium where their chemical potential is the same in all the domains. Hence, there should be a homogeneous distribution of the molecules within the BCP as seen for the 20% EG system for the extended solvent annealing time. In general, the insertion of the additive corresponds to the rearrangement of the blocks by the reduction of the interfacial tension which changes the stretching free energy (strain) of the system in order to maintain a constant packing density. The stretching free energy is also related to the distribution of the additive within the microdomain of the BCP and this will depend on the chain length. The stretching of the blocks will also be related to the interaction energy of the added polymer chain and the BCP microdomain chains. For a small additive of similar chemical structure to the domain polymers, in order to reduce interfacial strain energy of the BCP domains and additive-domain strain energies, the added molecules will tend to phase segregate at the interface (of the blocks) and act as a compatibilizer, thereby significantly decreasing the interfacial tension and increasing the stretching energy, resulting in a decrease of the equilibrium domain size after phase separation [18]. However, for longer chain

additives, most of the chains are localized in their corresponding bulk domain and act as homopolymer fillers, thus resulting in a smaller change in the interfacial tension along with a decrease in the stretching energy, and the additive can be viewed as a change in the BCP composition ensuing an overall increase in the equilibrium domain size after phase separation.

3.7. Discussion

In this work, several key observations were made that require detailed consideration using the concepts described above. Firstly, there are apparent changes of solubility limit for each of the glycol additives which result in changes of the periodicity (i.e. order). Secondly, changes in domain size with additive and concentration (both reductions and expansions were noted) were more complex than expected. Finally cyclical changes in cylinder orientation with solvent annealing time were seen with the glycol addition. These three factors are described further below.

For the EG and TEG systems, the effect of the additive appears to be dominated by small molecule (compatibilzer) effects since the domain separation is always less or equal to that of the unadulterated system (25 nm). This is most noticeable for the EG system which can attain domain sizes of as low as 16 nm. There is a kinetic effect for both the EG and TEG systems (although very much less pronounced for TEG) where the domain size reduces with solvent anneal time. This could be due to either phase separation from within the block or due to the mass transport of the additive through the PS matrix to the domain interface. For EG, similar kinetic effects are seen at 40% loadings but apparently with faster kinetics probably associated with the higher concentration and reduced mass transport requirements. This probably explains why the 70% EG, although dewetted, shows the minimum domain size.

For TEG and PEG, the domain spacing effects are much reduced. This is probably due to limited solubility. As seen above, the formation of overlayers was noted and it is suggested

that for both systems, the amount of material at the interface is reduced whilst there is greater tendency to be maintained within the bulk of the PEO block. Thus, there is a balance of bulk and comaptabilizer effects. In the case of PEG, there is obvious significant distribution within the bulk of the block as domain spacing increases to greater values than the unadulterated system. It should also be noted that there is a decreasing solubility limit with increased molecular weight. It could be conjectured that the solubility is defined by a combination of the available domain interface area (since this is the most energetically favourable position for small molecules) and the strain/chemical mis-match imposed by the additives in the bulk of the polymer block. Clearly, from the data, when the solubility limit is reached, material has to reach the surface-gas interface and this leads to dewetting as molecular interactions favour de-mixing [38].

The morphological orientation (i.e. vertical vs horizontal cylinder arrangements relative to the surface plane) requires discussion. The casting and annealing solvent play an important role in defining the cylinder orientation. The casting solvents used are different compositions of toluene and EG's. PEO is a semi-crystalline polymer and it is reasonable to presume that the crystalline fraction cannot interact easily with the additive [35]. The molecular mobility of the amorphous PEO is higher, thus it can be assumed that a large fraction of PEO is available (no crystallinity was observed in cross-sectional TEM after solvent annealing) for the dissolution with the additive at an elevated temperature [35]. This non-glassy/crystalline nature of the PEO block also suggests the kinetics of additive and the phase separation are limited by the PS matrix. Although PEO dissolves in toluene, the toluene is a selective solvent for PS since the solubility parameter difference with PS is much smaller ($\delta_{Tol} - \delta_{PS}$ = 18.3-18 =0.3 $MPa^{1/2}$) than PEO does ($\delta_{Tol} - \delta_{PEO}$ = 18.3-20.2 =1.9 $MPa^{1/2}$) [9]. Thus, toluene will selectively swell PS, increase the mobility of the PS chain matrix and sponsor self-assembly. Elevated temperature (50^0 C, toluene vapour pressure of 12.3 kPa) solvent

annealing is required since the vapour pressure of toluene at room temperature (0.0342 kPa) is not sufficient for swelling the entire film thickness [8]. Although 30 minutes of solvent exposure resulted in microphase separation, extended period solvent annealing are required to decrease the pattern defectivity and to ensure homogeneous mixing and interactions of the additives with the BCP. Note that exposure to water vapour is avoided to achieve long range ordered homogeneous film because sorption of water, with a reported glass transition temperature, T_g = -136^o C, [35] plasticize the amorphous regions of PEO thereby reducing the viscosity and increasing the molecular mobility of the microdomains. This leads to an increased defectivity in the phase separated nanostructures as well as tendency for the cylindrical morphology to flip from perpendicular to parallel [8]. For EG and TEG conditions appear to favour a vertical (to the surface plane) arrangement of cylinders and there is little sign of horizontal orientation whereas a cyclical rearrangement from vertical-to-parallel-to-vertical orientation were realized for the PEG mediated thin films as a function of solvent annealing time. The preference for the vertical cylinder orientation for these films can be explained by two possible effects. The first one constitutes a phenomenological argument [39] that a thermodynamic compensating force originated to favour the perpendicular cylinder arrangement due to considerable increase in the domain-matrix excess free energy during the reorientation of the cylinders from parallel to perpendicular. This favourable contribution could be enthalpic, originating from an increase of incompatibility, compared to the pristine BCP, between the matrix and the dispersed phase and/or from an intermolecular affinity between the additive and the corresponding block component [39]. The second one is the confinement of the additive to the centre of the cylinders inducing a stretching of the chains along the axis of the cylinders and this is more easily accommodated when the cylinders are aligned so they extend in the plane orthogonal to the surface plane [40]. It was reported that the blending of the PEO based BCP with some additives (homopolymers) could

induce an increase in incompatibility towards the other block [41-42]. Therefore, it is expected that the EG will be localized in the centre of the PEO cylinders in order to minimize the contacts with the PS matrix, moreover there is a strong affinity between PEO and EG. Thus, it can be concluded that a highly favourable enthalpic interaction between the PEO block and the small molecular chain of EG, i.e. enhanced compatibility leads to the perpendicular orientation of cylinders. The enrichment of the additives in the core of the cylindrical domains depends on the molecular weight or chain length of the additives. The enrichment starts from the centre and propagates as coaxial layering of PEO and additive [15]. The distribution of the additives within the BCP can further be explained in terms of entropy effects. The difference in degree of penetration into the copolymer block can be directly correlated to the relative translational and conformational entropy losses associated with the confinement of the short and long chain additives [43]. For shorter chains, the increase in translational entropy due to uniform solubilization in the domains compensates with the slight decrease in conformational entropy resulting from the stretching of the copolymer chains to create space for the additive. For the longer chains, however, the diblock chains would have to stretch appreciably to allow the additive chains to intermingle, resulting in a substantial decrease in conformational entropy of the diblock chains (more than could be gained from any increase in translational entropy of the additive chains), and as a result the additives locally segregate towards the centre of the microdomain instead of intermixing with the BCP [18]. This tendency with PEG is reflected in the swelling of the PEO microdomains noted in Table 1. Thus, at short annealing times, where the PEG is located through the film a vertical alignment is seen since the effective Flory-Huggins interaction parameter is reduced by the dispersion of the PEG. On more extended annealing, the PEG becomes predominantly located at the core of the PEO cylinders and the domain-domain interaction is increased and parallel orientation is favoured. On very extended annealing times, the PEG essentially phase

separates to the surface of the film and this forms an effective 'capping layer' that strongly favours PEO at the surface and so ordains a vertical alignment. The considerable increase in the pitch size with longer chain length additives is also a strong indication that the additives are not homogeneously distributed inside the PEO cylinders but instead segregated in the centre of the cylinders leads to significant swelling of the PEO microdomains. This is why the neat TEG and PEG IR bands were observed. This segregation effect become more intense by further increasing the volume fractions of the additives leads to local confinements. The parallel orientation is also favoured at the correct monolayer (relative to cylinder repeat distance) as the films are slightly thicker in this case. The cyclical flipping rate depends predominantly on the swelling and deswelling of the films by the sorption of annealing solvent [8].

The choice of the additives is also important here. Chemical structures of PEO monomers and tri/poly/ethylene glycol molecules (H-$(CH_2CH_2O)_n$-OH) are similar and it is asserted that during stirring, PEO chains are surrounded by the additive molecules but do not undergo any chemical interactions unless any externally applied or moulded-in tensile force (e.g. temperature) is applied. These additives can be represented as 'stress cracking agent' [44] as they do not cause any chemical degradation of the polymer structure but the local packing of the chain alters, leads to dimensional changes and alteration of physical properties. The degree of sorption of the additive into a semi-crystalline polymer such as PEO is strong as the amorphous phase exhibits higher chain mobility close to the T_g value, increases free volume resulting swelling effect, facilitates additive permeation into the polymer. This behaviour is strongly dependent on the concentration of the additive, exposure temperature, exposure time and most of all, the level of strain on/in the polymer [45-46]. Similar chemical structure, solubility parameters, amorphous nature, low T_g value of the PEO facilitates the alteration process. Also, chemical inertness of the PS matrix component of the BCP to the additives

holds the ordered structure after phase separation. At same temperature, the longer chain length additives affect the PEO molecules faster and induce higher order mobility, thereby pitch size modifies more rapidly compared to EG and causes frequent cylinder reorientations.

In this way, it can be seen that the addition of even simple (i.e. similar chemical nature to one of the blocks) molecular additives is far from facile and effects can be complex. Understanding the effects of these additives in block copolymer film arrangements and domain sizes is a challenge. In this work, it is shown that glycol additives of differing molecular weights can be used to control domain spacing between 16 and 31 nm. The location of the additive and its effect on the effective domain-domain interactions require careful consideration. However, such control of domain spacing might be extremely useful.

4. Conclusions

The morphological and structural behaviour of hexagonal phase PS-b-PEO with an additive of similar chemical structure to the PEO block (lower molecular weight poly/ethylene glycols) at different concentrations is investigated [13, 15-19]. It is shown here that well ordered hexagonally arranged phase segregated cylindrical phase BCP nanopatterns were obtained for solvent annealed films. Previous literature reports that microdomain spacing increases or is unaltered by blending the homopolymers or surfactants [20-22] and this might be expected here. However, the addition of glycols shows more complex behaviour including an unusual domain spacing reduction. We believe that these data demonstrates an attractive route by which the microdomain spacing can be ‘tuned’ to precise values using an additive and avoiding re-engineering of the block copolymer composition and molecular weight. In this system we can attain domain spacing in the range of 16-31 nm.

As well as the practical advantages (in applications such as block copolymer lithography), [1] the data suggest a complex chemistry arising from interfacial effects between the additive and the nanostructured BCP. The observed behaviour of unusual alteration in the domain

spacing is due to distribution of the additive through the BCP arrangement which is sensitive to concentration and the molecular weight of the additive. Although the chemical structures of PEO monomers and tri/poly/ethylene glycol molecules are similar, their cohesive energies are sensitive to their molecular weight. Their size might also be important in terms of steric effects. It is clear that the smaller molecular weight glycols can exist primarily at the domain-domain interface thereby increasing the stretching free energy of the system leading to a decrease in the pitch size whereas larger chain length additives segregated at the centre of the microdomain and consequently increases the microdomain spacing of the BCP. A compensating effect between the translational and conformational entropy between the polymer blocks and additive also causes the alteration in the microdomain spacing. The PEO cylinder orientation remains unchanged by smaller chain length EG's whereas cyclical reorientation was observed for the higher chain length PEG due to the interplay of PEO block-additive segregation and mirophase separation.

AUTHOR INFORMATION

Corresponding Authors

*Email: m.morris@ucc.ie; g_tandra@yahoo.co.in

Notes

The authors declare no competing financial interest.

Acknowledgements

We acknowledge financial support from the Science Foundation Ireland (Grants: Semiconductor Research Corporation 2011-IN-2194, 09/SIRG/I1621 and CSET CRANN). The contribution of the Foundation's Principal Investigator support is also acknowledged.

References

[1] Emerging Research Devices. In The International Technology Roadmap for Semiconductors, 2011; pp 1.

[2] R. Ruiz, H. M. Kang, F. A. Detcheverry, E. Dobisz, D. S. Kercher, T. R. Albrecht, J. J. de Pablo, P. F. Nealey, Science 321 (2008) 936.

[3] J. Y. Cheng, D. P. Sanders, H. D. Truong, S. Harrer, A. Friz, S. Holmes, M. Colburn, W. D. Hinsberg, ACS Nano 4 (2010) 4815.

[4] D. Borah, M. Ozmen, S. Rasappa, M. T. Shaw, J. D. Holmes, M. A. Morris, Langmuir 29 (2013) 2809.

[5] Q. Wang, P. F. Nealey, J. J. de Pablo, Macromolecules 34 (2001) 3458.

[6] S. Rasappa, D. Borah, C. C. Faulkner, T. Lutz, M. T. Shaw, J. D. Holmes, M. A. Morris, Nanotechnology 24 (2013).

[7] D. Borah, M. T. Shaw, S. Rasappa, R. A. Farrell, C. O'Mahony, C. M. Faulkner, M. Bosea, P. Gleeson, J. D. Holmes, M. A. Morris, J. Phys. D-Appl. Phys. 44 (2011) 174012.

[8] P. Mokarian-Tabari, T. W. Collins, J. D. Holmes, M. A. Morris, ACS Nano 5 (2011) 4617.

[9] T. M. Ghoshal, T; Senthamaraikannan, R; Shaw, M; Carolan, P; Holmes, J; Roy, S; Morris, M, Scientific Reports 3 (2013) 2772.

[10] J. C. Zhao, S. C. Jiang, X. L. Ji, L. J. An, B. Z. Jiang, Polymer 46 (2005) 6513.

[11] S. W. Hong, W. Gu, J. Huh, B. R. Sveinbjornsson, G. Jeong, R. H. Grubbs, T. P. Russell, ACS Nano 7 (2013) 9684.

[12] J. Bodycomb, D. Yamaguchi, T. Hashimoto, Macromolecules 33 (2000) 5187.

[13] K. I. Winey, E. L. Thomas, L. J. Fetters, Macromolecules 25 (1992) 2645.

[14] N. Hameed, J. Liu, Q. P. Guo, Macromolecules 41 (2008) 7596.

[15] N. Lefevre, K. C. Daoulas, M. Muller, J. F. Gohy, C. A. Fustin, Macromolecules 43 (2010) 7734.

[16] K. J. Jeon, R. J. Roe, Macromolecules 27 (1994) 2439.

[17] T. Hashimoto, H. Tanaka, H. Hasegawa, Macromolecules 23 (1990) 4378.

[18] J. Peng, X. Gao, Y. H. Wei, H. F. Wang, B. Y. Li, Y. C. Han, J. Chem. Phys. 122 (2005).

[19] K. I. Winey, E. L. Thomas, L. J. Fetters, Macromolecules 24 (1991) 6182.

[20] D. Yamaguchi, J. Bodycomb, S. Koizumi, T. Hashimoto, Macromolecules 32 (1999) 5884.

[21] U. Jeong, D. Y. Ryu, D. H. Kho, D. H. Lee, J. K. Kim, T. P. Russell, Macromolecules 36 (2003) 3626.

[22] M. D. Smith, P. F. Green, R. Saunders, Macromolecules 32 (1999) 8392.

[23] W. H. Huang, P. Y. Chen, S. H. Tung, Macromolecules 45 (2012) 1562.

[24] J. Peng, D. H. Kim, W. Knoll, Y. Xuan, B. Y. Li, Y. C. Han, J. Chem. Phys. 125 (2006).

[25] H. Kitano, S. Akasaka, T. Inoue, F. Chen, M. Takenaka, H. Hasegawa, H. Yoshida, H. Nagano, Langmuir 23 (2007) 6404.

[26] C. B. Tang, E. M. Lennon, G. H. Fredrickson, E. J. Kramer, C. J. Hawker, Science 322 (2008) 429.

[27] J. Bang, U. Jeong, D. Y. Ryu, T. P. Russell, C. J. Hawker, Adv. Mater. 21 (2009) 4769.

[28] T. Ghoshal, T. Maity, J. F. Godsell, S. Roy, M. A. Morris, Adv. Mater. 24 (2012) 2390.

[29] W. Y. Chen, J. X. Zheng, S. Z. D. Cheng, C. Y. Li, P. Huang, L. Zhu, H. M. Xiong, Q. Ge, Y. Guo, R. P. Quirk, B. Lotz, L. F. Deng, C. Wu, E. L. Thomas, Phys. Rev. Lett. 93 (2004) 028301.

[30] G. H. Michler, Electron Microscopy of Polymers Springer: 2008.

[31] K. Ibrahim, A. Salminen, S. Holappa, K. Kataja, H. Lampinen, B. Lofgren, J. Laine, J. Seppala, J. Appl. Polym. Sci. 102 (2006) 4304.

[32] F. Ahmad, M. K. Baloch, M. Jamil, Y. J. Jeon, J. Appl. Polym. Sci. 118 (2010) 1704.

[33] J. J. Tunney, C. Detellier, Clay Clay Min. 42 (1994) 552.

[34] S. Biswal, J. Sahoo, P. N. Murthy, R. P. Giradkar, J. G. Avari, AAPS PharmSciTech 9 (2008) 563.

[35] P. J. Marsac, D. P. Romary, S. L. Shamblin, J. A. Baird, L. S. Taylor, J. Pharm. Sci. 97 (2008) 3182.

[36] A. C. Shi, J. Noolandi, Macromolecules 27 (1994) 2936.

[37] T. Ghoshal, M. T. Shaw, C. T. Bolger, J. D. Holmes, M. A. Morris, J. Mater. Chem. 22 (2012) 12083.

[38] C. E. Sing, J. W. Zwanikken, M. O. de la Cruz, Nat. Mater. 13 (2014) 694.

[39] D. U. Ahn, E. Sancaktar, Adv. Funct. Mater. 16 (2006) 1950.

[40] U. Jeong, D. Y. Ryu, D. H. Kho, J. K. Kim, J. T. Goldbach, D. H. Kim, T. P. Russell, Adv. Mater. 16 (2004) 533.

[41] V. R. Tirumala, V. Daga, A. W. Bosse, A. Romang, J. Ilavsky, E. K. Lin, J. J. Watkins, Macromolecules 41 (2008) 7978.

[42] S. H. Kim, M. J. Misner, L. Yang, O. Gang, B. M. Ocko, T. P. Russell, Macromolecules 39 (2006) 8473.

[43] K. A. Orso, P. F. Green, Macromolecules 32 (1999) 1087.

[44] P. Neogi, G. Zahedi, Ind. Eng. Chem. Res. 53 (2014) 672.

[45] A. Opdahl, G. A. Somorjai, J. Polym. Sci. Pt. B-Polym. Phys. 39 (2001) 2263.

[46] C. P. Lafrance, P. Chabot, M. Pigeon, R. E. Prudhomme, M. Pezolet, Polymer 34 (1993) 5029.

Figure captions:

Fig. 1. Tapping mode AFM images of the phase segregated thin films of mixture of PS-b-PEO and 20% weight fraction of EG solvent annealed in toluene at 50^{o} C for different time (a) 30 m (b) 1 h (c) 1 h 30 m (d) 2 h (e) 2 h 30 m (f) 3 h.

Fig. 2. Tapping mode AFM images of the phase segregated thin films of mixture of PS-b-PEO and 20% weight fraction of TEG solvent annealed in toluene at 50^{o} C for different time (a) 30 m (b) 1 h (c) 1 h 30 m (d) 2 h (e) 2 h 30 m (f) 3 h.

Fig. 3. Tapping mode AFM images of the phase segregated thin films of mixture of PS-b-PEO and 20% weight fraction of PEG solvent annealed in toluene at 50^{o} C for different time (a) 30 m (b) 1 h (c) 1 h 30 m (d) 2 h (e) 2 h 30 m (f) 3 h.

Fig. 4. (a) Top-down and (b) cross-sectional SEM images of the phase segregated thin films of mixture of PS-b-PEO and 20% weight fraction of EG solvent annealed in toluene at 50^{o} C for 3h after partial oxygen plasma PEO etch.

Fig. 5. Cross-sectional TEM image of the phase segregated thin films of mixture of PS-b-PEO and 20% weight fraction of EG solvent annealed in toluene at 50^{o} C for 3h after partial oxygen plasma PEO etch.

Fig. 6. FTIR spectra of the phase segregated thin films of mixture of PS-b-PEO and 20% weight fraction of EG, TEG and PEG, solvent annealed in toluene at 50^{o} C for 3h.

Table 1. Morphology and pitch size variation of the solvent annealed films for different concentrations of additives with annealing time

Additive	Concentrations (wt%)	Annealing time (min)	Morphology	Pitch size (nm)
EG	20	30	dots	25 ± 3
EG	20	60	dots	23 ± 4
EG	20	90	dots	20 ± 6
EG	20	120	dots	17 ± 6
EG	20	150	dots	16 ± 3
EG	20	180	dots	16 ± 2
EG	40	30	dots	23 ± 6
EG	40	60	dots	18 ± 6
EG	40	90-180	Dots, dewetting	16 ± 6
EG	70	60-180	dewetting	16 ± 8
TEG	20	30	dots	25 ± 3
TEG	20	60	dots	22 ± 4
TEG	20	90	dots	21 ± 5
TEG	20	120	dots	21 ± 6
TEG	20	150	dots	20 ± 6
TEG	20	180	dots	20 ± 6
TEG	40-70	60-180	dewetting	-
PEG	20	30	dots	27 ± 3
PEG	20	60	Dots + Fingerprint	29 ± 4
PEG	20	90	lines	30 ± 3
PEG	20	120	lines	31 ± 3
PEG	20	150	Dots + Fingerprint	31 ± 7
PEG	20	180	dots	31 ± 5
PEG	40-70	60-180	dewetting	-

Supporting Information:

Morphology of the solvent annealed film for different concentrations of EG.

Fig. S1 shows the topographic images of the solvent annealed film for different concentrations of EG after solvent annealing in toluene for 1h. For 40%, the hexagonal dot patterns were observed for the annealing time of 1h. But further increasing the annealing time local confinement of the dot patterns with film dewetting obtained. Serious dewetting observed for 70% concentrations of EG with the dot patterns only in few areas.

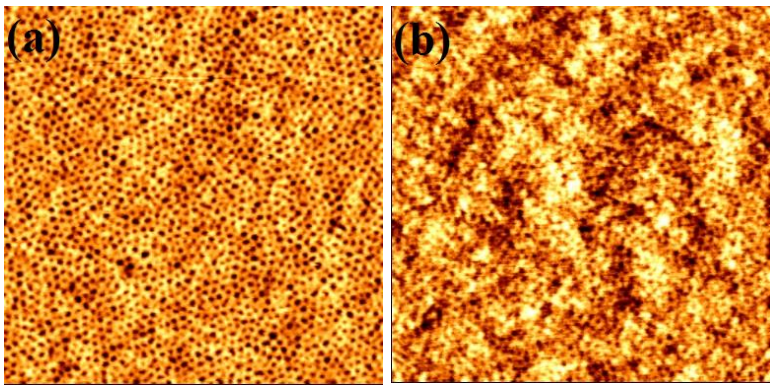

Fig. S1. Tapping mode AFM images of the phase segregated thin films of mixture of PS-b-PEO with a weight fraction of (a) 40% and (b) 70% EG solvent annealed in toluene at 50^{o} C for 1 h.

Pitch size variation with solvent annealing time for different additives.

Fig. S2 shows the pitch size variation with solvent annealing time for different additives. For the EG, the uniformity in the dot size increases with the annealing time with a very small deviation whereas larger deviation was observed for TEG. For PEG, the pitch size is uniform for smaller annealing time compared to increase in annealing times.

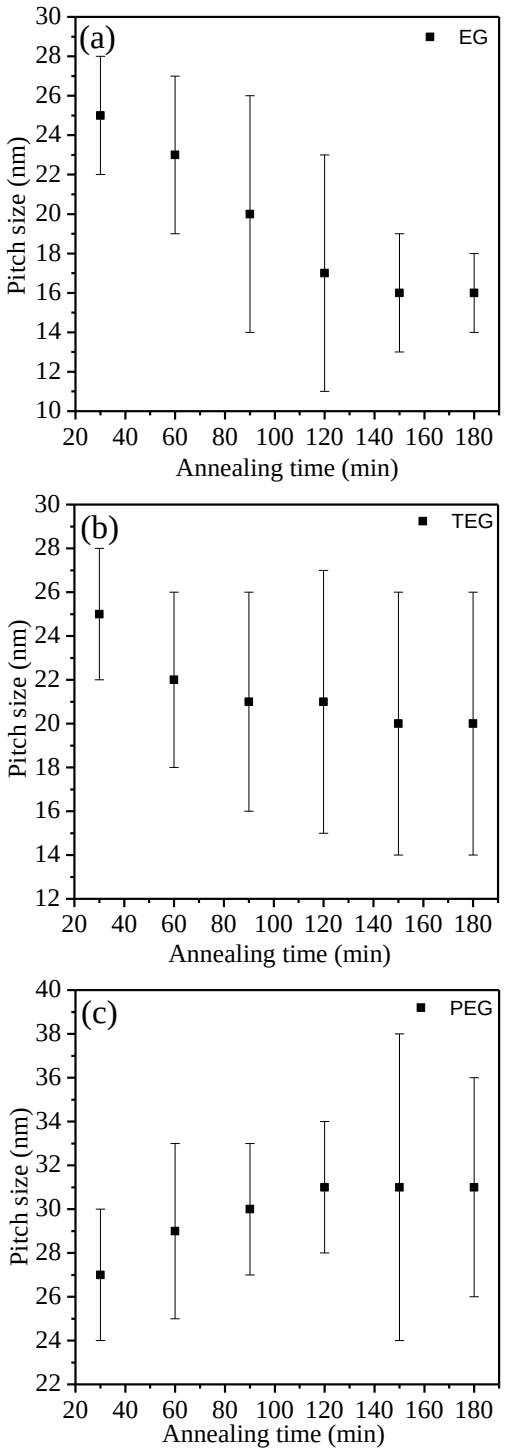

Fig. S2. Pitch size variation with solvent annealing time for different additives (a) EG, (b) TEG and (c) PEG.

5: Figure 1

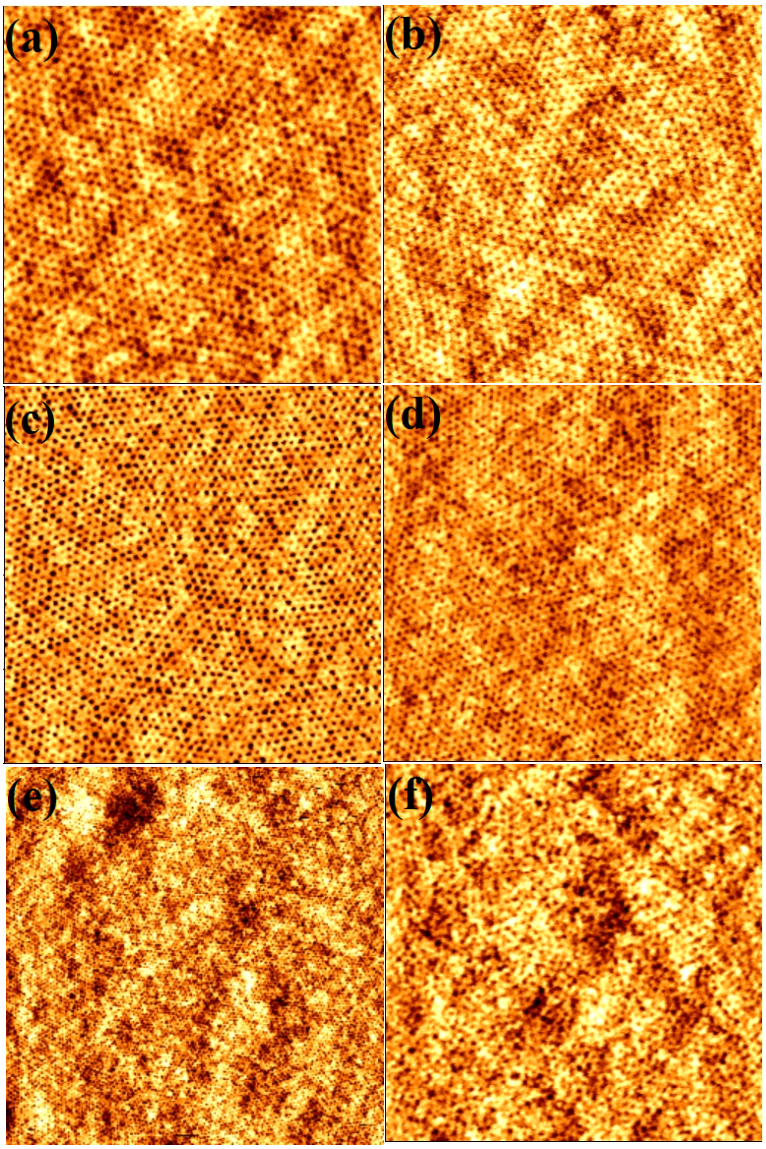

Fig. 1

5: Figure 2

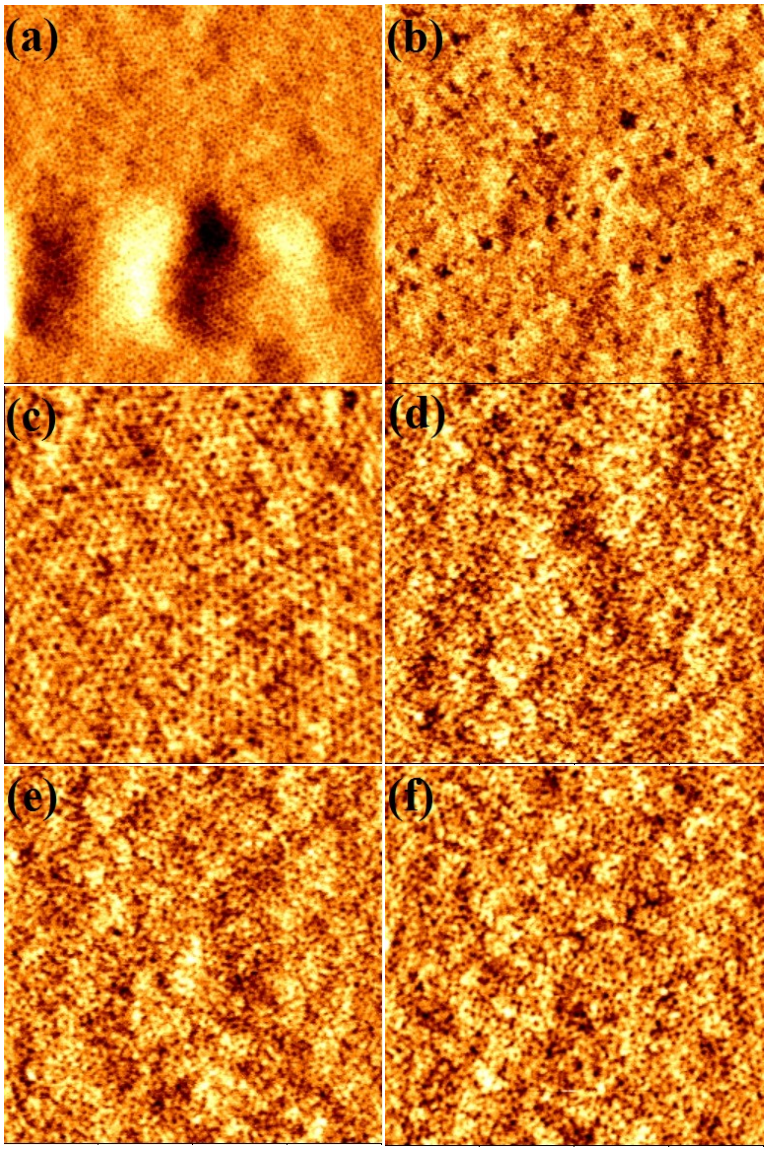

Fig. 2

5: Figure 3

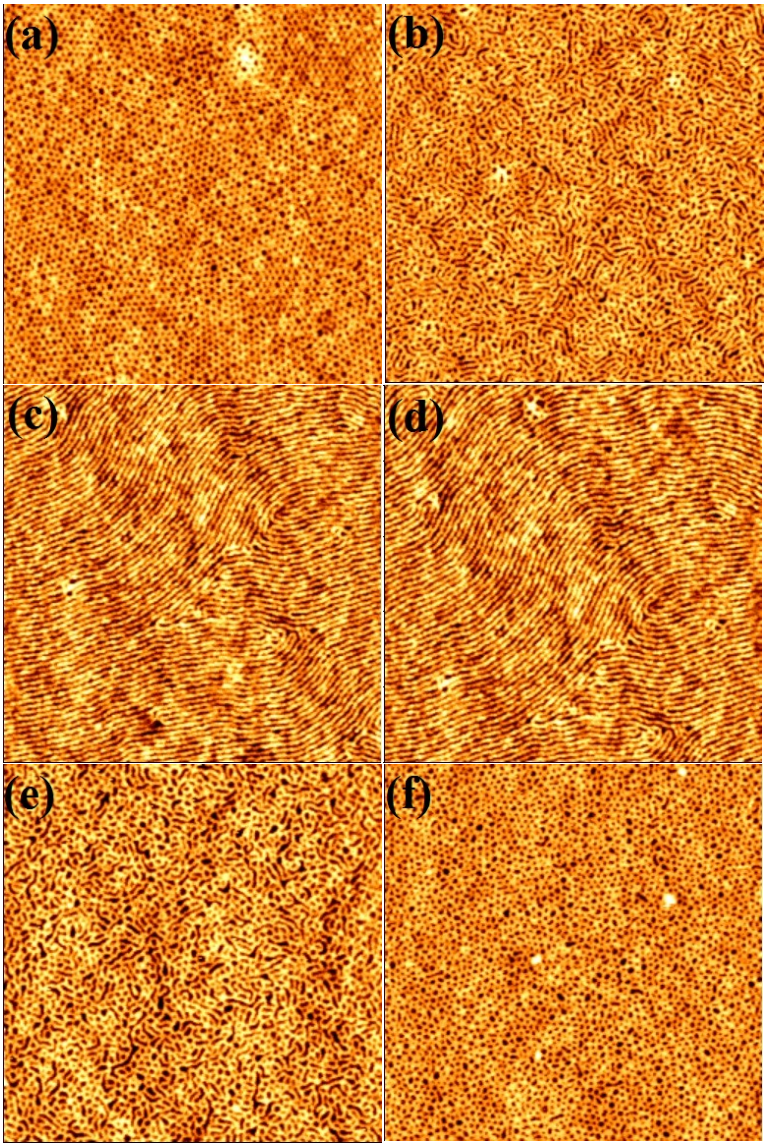

Fig. 3

5: Figure 4

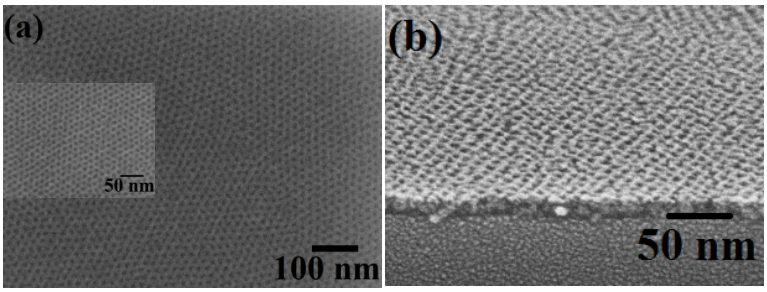

Fig. 4

Figure 5

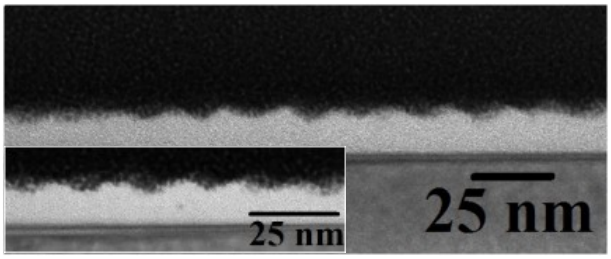

Fig. 5

5: Figure 6

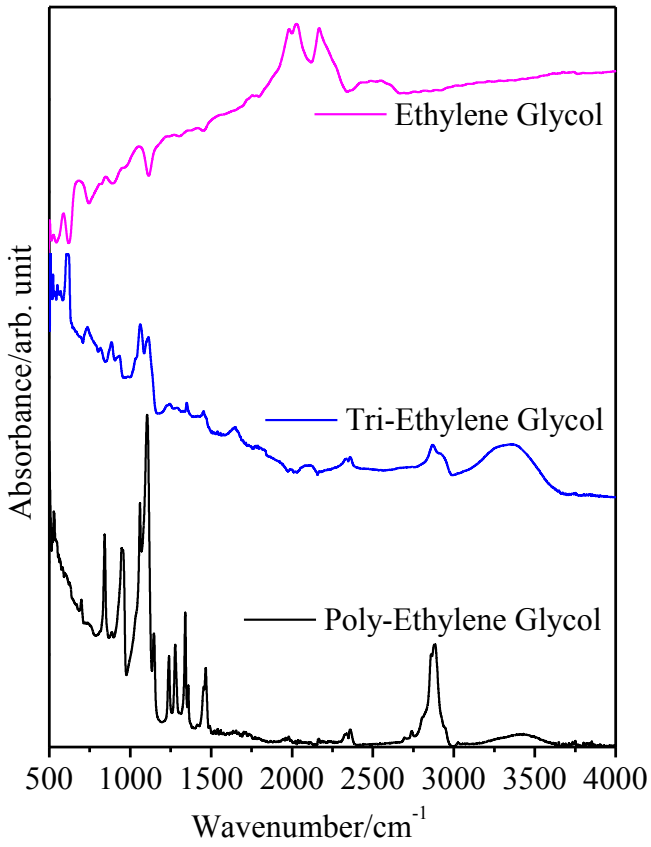

Fig. 6

6: Table

Table 1. Morphology and pitch size variation of the solvent annealed films for different concentrations of additives with annealing time

Additive	Concentrations (wt%)	Annealing time (min)	Morphology	Pitch size (nm)
EG	20	30	dots	25 ± 3
EG	20	60	dots	23 ± 4
EG	20	90	dots	20 ± 6
EG	20	120	dots	17 ± 6
EG	20	150	dots	16 ± 3
EG	20	180	dots	16 ± 2
EG	40	30	dots	23 ± 6
EG	40	60	dots	18 ± 6
EG	40	90-180	Dots, dewetting	16 ± 6
EG	70	60-180	dewetting	16 ± 8
TEG	20	30	dots	25 ± 3
TEG	20	60	dots	22 ± 4
TEG	20	90	dots	21 ± 5
TEG	20	120	dots	21 ± 6
TEG	20	150	dots	20 ± 6
TEG	20	180	dots	20 ± 6
TEG	40-70	60-180	dewetting	-
PEG	20	30	dots	27 ± 3
PEG	20	60	Dots + Fingerprint	29 ± 4
PEG	20	90	lines	30 ± 3
PEG	20	120	lines	31 ± 3
PEG	20	150	Dots + Fingerprint	31 ± 7
PEG	20	180	dots	31 ± 5
PEG	40-70	60-180	dewetting	-

7: Electronic Supplementary Material (online publication only)

Click here to download 7: Electronic Supplementary Material (online publication only): Supporting Information.docx